EUROPEAN ORGANIZATION FOR NUCLEAR RESEARCH

CERN-PPE/91-213

3 December 1991

A Measurement of the $b\bar{b}$ Forward Backward Asymmetry Using the Semileptonic Decay into Muons

DELPHI Collaboration

Abstract

The forward backward asymmetry of bottom quarks is measured with statistics of approximately 80 000 hadronic Z°-decays produced in e^+e^--collisions at a centre of mass energy of $\sqrt{s} \approx M_Z$. The tagging of b-quark events has been performed using the semileptonic decay channel $b \to X + \mu$. Because the asymmetry depends on the weak coupling, this leads to a precise measurement of the electroweak mixing angle $\sin^2\theta_W$. The experimental result is $A_{FB}^b = 0.115 \pm 0.043\,(stat) \pm 0.013\,(syst)$. After correcting the value for the $B^0\bar{B}^0$-mixing this becomes $A_{FB}^b = 0.161 \pm 0.060\,(stat) \pm 0.021\,(syst)$ corresponding to $\sin^2\theta_W^{\overline{MS}} = 0.221 \pm 0.011\,(stat) \pm 0.004\,(syst)$.

(Submitted to Phys. Lett. B)

P.Abreu[18], W.Adam[43], F.Adami[34], T.Adye[32], T.Akesson[21], G.D.Alekseev[13], P.Allen[42], S.Almehed[21], S.J.Alvsvaag[4], U.Amaldi[7], E.Anassontzis[3], P.Antilogus[22], W-D.Apel[14], R.J.Apsimon[32], B.Åsman[38], J-E.Augustin[16], A.Augustinus[27], P.Baillon[7], P.Bambade[16], F.Barao[18], R.Barate[11], G.Barbiellini[40], D.Y.Bardin[13], A.Baroncelli[35], O.Barring[21], W.Bartl[43], M.J.Bates[30], M.Battaglia[25], M.Baubillier[20], K-H.Becks[45], C.J.Beeston[30], M.Begalli[10], P.Beilliere[6], Yu.Belokopytov[37], P.Beltran[9], D.Benedic[8], J.M.Benlloch[42], M.Berggren[16], D.Bertrand[2], F.Bianchi[39], M.S.Bilenky[13], P.Billoir[20], J.Bjarne[21], D.Bloch[8], S.Blyth[30], V.Bocci[33], P.N.Bogolubov[13], T.Bolognese[34], M.Bonapart[27], M.Bonesini[25], W.Bonivento[25], P.S.L.Booth[19], P.Borgeaud[34], G.Borisov[37], H.Borner[7], C.Bosio[35], B.Bostjancic[7], O.Botner[41], B.Bouquet[16], C.Bourdarios[16], M.Bozzo[10], S.Braibant[2], P.Branchini[35], K.D.Brand[31], R.A.Brenner[12], H.Briand[20], C.Bricman[2], R.C.A.Brown[7], N.Brummer[27], J-M.Brunet[6], L.Bugge[29], T.Buran[29], H.Burmeister[7], J.A.M.A.Buytaert[7], M.Caccia[7], M.Calvi[25], A.J.Camacho Rozas[36], A.Campion[19], T.Camporesi[7], V.Canale[33], F.Cao[2], F.Carena[7], L.Carroll[19], C.Caso[10], E.Castelli[40], M.V.Castillo Gimenez[42], A.Cattai[7], F.R.Cavallo[5], L.Cerrito[33], A.Chan[1], M.Chapkin[37], P.Charpentier[7], L.Chaussard[16], J.Chauveau[20], P.Checchia[31], G.A.Chelkov[13], L.Chevalier[34], P.Chliapnikov[37], V.Chorowicz[20], R.Cirio[39], M.P.Clara[39], P.Collins[30], J.L.Contreras[23], R.Contri[10], G.Cosme[16], F.Couchot[16], H.B.Crawley[1], D.Crennell[32], G.Crosetti[10], M.Croson[6], J.Cuevas Maestro[36], S.Czellar[12], S.Dagoret[16], E.Dahl-Jensen[26], B.Dalmagne[16], M.Dam[29], G.Damgaard[26], G.Darbo[10], E.Daubie[2], P.D.Dauncey[30], M.Davenport[7], P.David[20], W.Da Silva[20], C.Defoix[6], D.Delikaris[7], S.Delorme[7], P.Delpierre[6], N.Demaria[39], A.De Angelis[40], M.De Beer[34], H.De Boeck[2], W.De Boer[14], C.De Clercq[2], M.D.M.De Fez Laso[42], N.De Groot[27], C.De La Vaissiere[20], B.De Lotto[40], A.De Min[25], H.Dijkstra[7], L.Di Ciaccio[33], F.Djama[8], J.Dolbeau[6], M.Donszelmann[27], K.Doroba[44], M.Dracos[7], J.Drees[45], M.Dris[28], Y.Dufour[6], W.Dulinski[8], R.Dzhelyadin[37], L-O.Eek[41], P.A.-M.Eerola[7], T.Ekelof[41], G.Ekspong[38], A.Elliot Peisert[31], J-P.Engel[8], D.Fassouliotis[28], M.Feindt[7], M.Fernandez Alonso[36], A.Ferrer[42], T.A.Filippas[28], A.Firestone[1], H.Foeth[7], E.Fokitis[28], P.Folegati[40], F.Fontanelli[10], K.A.J.Forbes[19], B.Franek[32], P.Frenkiel[6], D.C.Fries[14], A.G.Frodesen[4], R.Fruhwirth[43], F.Fulda-Quenzer[16], K.Furnival[19], H.Furstenau[14], J.Fuster[7], G.Galeazzi[31], D.Gamba[39], C.Garcia[42], J.Garcia[36], C.Gaspar[7], U.Gasparini[31], P.Gavillet[7], E.N.Gazis[28], J-P.Gerber[8], P.Giacomelli[7], R.Gokieli[7], V.M.Golovatyuk[13], J.J.Gomez Y Cadenas[7], A.Goobar[38], G.Gopal[32], M.Gorski[44], V.Gracco[10], A.Grant[7], F.Grard[2], E.Graziani[35], G.Grosdidier[16], E.Gross[7], P.Grosse-Wiesmann[7], B.Grossetete[20], S.Gumenyuk[37], J.Guy[32], F.Hahn[7], M.Hahn[14], S.Haider[27], Z.Hajduk[15], A.Hakansson[21], A.Hallgren[41], K.Hamacher[45], G.Hamel De Monchenault[34], F.J.Harris[30], B.W.Heck[7], T.Henkes[7], J.J.Hernandez[42], P.Herquet[2], H.Herr[7], I.Hietanen[12], C.O.Higgins[19], E.Higon[42], H.J.Hilke[7], S.D.Hodgson[30], T.Hofmokl[44], R.Holmes[1], S-O.Holmgren[38], D.Holthuizen[27], P.F.Honore[6], J.E.Hooper[26], M.Houlden[19], J.Hrubec[43], P.O.Hulth[38], K.Hultqvist[38], D.Husson[8], P.Ioannou[3], D.Isenhower[7], P-S.Iversen[4], J.N.Jackson[19], P.Jalocha[15], G.Jarlskog[21], P.Jarry[34], B.Jean-Marie[16], E.K.Johansson[38], D.Johnson[19], M.Jonker[7], L.Jonsson[21], P.Juillot[8], G.Kalkanis[3], G.Kalmus[32], F.Kapusta[20], M.Karlsson[7], S.Katsanevas[3], E.C.Katsoufis[28], R.Keranen[12], J.Kesteman[2], B.A.Khomenko[13], N.N.Khovanski[13], B.King[19], N.J.Kjaer[7], H.Klein[7], W.Klempt[7], A.Klovning[4], P.Kluit[27], J.H.Koehne[14], B.Koene[27], P.Kokkinias[9], M.Kopf[14], M.Koratzinos[39], K.Korcyl[15], A.V.Korytov[13], V.Kostiukhin[37], C.Kourkoumelis[3], P.H.Kramer[45], T.Kreuzberger[43], J.Krolikowski[44], I.Kronkvist[21], J.Krstic[30], U.Kruener-Marquis[45], W.Krupinski[15], W.Kucewicz[25], K.Kurvinen[12], C.Lacasta[42], C.Lambropoulos[9], J.W.Lamsa[1], L.Lanceri[40], V.Lapin[37], J-P.Laugier[34], R.Lauhakangas[12], G.Leder[43], F.Ledroit[11], R.Leitner[7], Y.Lemoigne[34], J.Lemonne[2], G.Lensen[45], V.Lepeltier[16], A.Letessier-Selvon[20], E.Lieb[45], D.Liko[43], E.Lillethun[4], J.Lindgren[12], R.Lindner[45], A.Lipniacka[44], I.Lippi[31], R.Llosa[23], B.Loerstad[21], M.Lokajicek[13], J.G.Loken[30], A.Lopez-Fernandez[16], M.A.Lopez Aguera[36], M.Los[27], D.Loukas[9], A.Lounis[8], J.J.Lozano[42], P.Lutz[6], L.Lyons[30], G.Maehlum[7], J.Maillard[6], A.Maltezos[9], F.Mandl[43], J.Marco[36], M.Margoni[31], J-C.Marin[7], A.Markou[9], T.Maron[45], S.Marti[42], L.Mathis[1], F.Matorras[36], C.Matteuzzi[25], G.Matthiae[33], M.Matveev[37], M.Mazzucato[31], M.Mc Cubbin[19], R.Mc Kay[1], R.Mc Nulty[19], E.Menichetti[39], G.Meola[10], C.Meroni[25], W.T.Meyer[1], M.Michelotto[31], W.A.Mitaroff[43], G.V.Mitselmakher[13], U.Mjoernmark[21], T.Moa[38], R.Moeller[26], K.Moenig[7], M.R.Monge[10], P.Morettini[10], H.Mueller[14], W.J.Murray[32], B.Muryn[16], G.Myatt[30], F.Naraghi[20], F.L.Navarria[5], P.Negri[25], B.S.Nielsen[26], B.Nijjhar[19], V.Nikolaenko[37], V.Obrastsov[37], K.Oesterberg[12], A.G.Olshevski[13], R.Orava[12], A.Ostankov[37], A.Ouraou[34], M.Paganoni[25], R.Pain[20], H.Palka[27], T.Papadopoulou[28], L.Pape[7], A.Passeri[35], M.Pegoraro[31], J.Pennanen[12], V.Perevoschikov[37], M.Pernicka[43], A.Perrotta[5], F.Pierre[34], M.Pimenta[18], O.Pingot[2], M.E.Pol[7], G.Polok[15], P.Poropat[40], P.Privitera[14], A.Pullia[25], D.Radojicic[30], S.Ragazzi[25], P.N.Ratoff[17], A.L.Read[29], N.G.Redaelli[25], M.Regler[43], D.Reid[19], P.B.Renton[30], L.K.Resvanis[3], F.Richard[16], M.Richardson[19], J.Ridky[13], G.Rinaudo[39], I.Roditi[7], A.Romero[39], I.Roncagliolo[10], P.Ronchese[31], C.Ronnqvist[12], E.I.Rosenberg[1], U.Rossi[5], E.Rosso[7], P.Roudeau[16], T.Rovelli[5], W.Ruckstuhl[27], V.Ruhlmann[34], A.Ruiz[36], K.Rybicki[15], H.Saarikko[12], Y.Sacquin[34], G.Sajot[11], J.Salt[42], E.Sanchez[42], J.Sanchez[23], M.Sannino[10], M.Schaeffer[8], S.Schael[14], H.Schneider[14], M.A.E.Schyns[45], F.Scuri[40], A.M.Segar[30], R.Sekulin[32], M.Sessa[40], G.Sette[10], R.Seufert[14], R.C.Shellard[7], P.Siegrist[34], S.Simonetti[10], F.Simonetto[31], A.N.Sissakian[13], T.B.Skaali[29], G.Skjevling[29], G.Smadja[34,22], N.Smirnov[37], G.R.Smith[32], R.Sosnowski[44], T.S.Spassoff[11], E.Spiriti[35],

S.Squarcia[10], H.Staeck[45], C.Stanescu[35], G.Stavropoulos[9], F.Stichelbaut[2], A.Stocchi[16], J.Strauss[43], R.Strub[8], M.Szczekowski[44], M.Szeptycka[44], P.Szymanski[44], T.Tabarelli[25], S.Tavernier[2], G.E.Theodosiou[9], A.Tilquin[24], J.Timmermans[27], V.G.Timofeev[13], L.G.Tkatchev[13], T.Todorov[13], D.Z.Toet[27], O.Toker[12], E.Torassa[39], L.Tortora[35], M.T.Trainor[30], D.Treille[7], U.Trevisan[10], W.Trischuk[7], G.Tristram[6], C.Troncon[25], A.Tsirou[7], E.N.Tsyganov[13], M.Turala[15], R.Turchetta[8], M-L.Turluer[34], T.Tuuva[12], I.A.Tyapkin[13], M.Tyndel[32], S.Tzamarias[7], S.Ueberschaer[45], O.Ullaland[7], V.Uvarov[37], G.Valenti[5], E.Vallazza[39], J.A.Valls Ferrer[42], C.Vander Velde[2], G.W.Van Apeldoorn[27], P.Van Dam[27], W.K.Van Doninck[2], J.Varela[18], P.Vaz[7], G.Vegni[25], L.Ventura[31], W.Venus[32], F.Verbeure[2], L.S.Vertogradov[13], D.Vilanova[34], L.Vitale[40], E.Vlasov[37], S.Vlassopoulos[28], A.S.Vodopyanov[13], M.Vollmer[45], S.Volponi[5], G.Voulgaris[3], M.Voutilainen[12], V.Vrba[35], H.Wahlen[45], C.Walck[38], F.Waldner[40], M.Wayne[1], A.Wehr[45], M.Weierstall[45], P.Weilhammer[7], J.Werner[45], A.M.Wetherell[7], J.H.Wickens[2], J.Wikne[29], G.R.Wilkinson[30], W.S.C.Williams[30], M.Winter[8], D.Wormald[29], G.Wormser[16], K.Woschnagg[41], N.Yamdagni[38], P.Yepes[7], A.Zaitsev[37], A.Zalewska[15], P.Zalewski[16], D.Zavrtanik[7], E.Zevgolatakos[9], G.Zhang[45], N.I.Zimin[13], M.Zito[34], R.Zitoun[20], R.Zukanovich Funchal[6], G.Zumerle[31], J.Zuniga[42]

[1] Ames Laboratory and Department of Physics, Iowa State University, Ames IA 50011, USA
[2] Physics Department, Univ. Instelling Antwerpen, Universiteitsplein 1, B-2610 Wilrijk, Belgium
and IIHE, ULB-VUB, Pleinlaan 2, B-1050 Brussels, Belgium
and Service de Phys. des Part. Elém., Faculté des Sciences, Université de l'Etat Mons, Av. Maistriau 19, B-7000 Mons, Belgium
[3] Physics Laboratory, University of Athens, Solonos Str. 104, GR-10680 Athens, Greece
[4] Department of Physics, University of Bergen, Allégaten 55, N-5007 Bergen, Norway
[5] Dipartimento di Fisica, Università di Bologna and INFN, Via Irnerio 46, I-40126 Bologna, Italy
[6] Collège de France, Lab. de Physique Corpusculaire, 11 pl. M. Berthelot, F-75231 Paris Cedex 05, France
[7] CERN, CH-1211 Geneva 23, Switzerland
[8] Division des Hautes Energies, CRN - Groupe DELPHI and LEPSI, B.P.20 CRO, F-67037 Strasbourg Cedex, France
[9] Institute of Nuclear Physics, N.C.S.R. Demokritos, P.O. Box 60228, GR-15310 Athens, Greece
[10] Dipartimento di Fisica, Università di Genova and INFN, Via Dodecaneso 33, I-16146 Genova, Italy
[11] Institut des Sciences Nucléaires, Université de Grenoble 1, F-38026 Grenoble, France
[12] Research Institute for High Energy Physics, University of Helsinki, Siltavuorenpenger 20 C, SF-00170 Helsinki 17, Finland
[13] Joint Institute for Nuclear Research, Dubna, Head Post Office, P.O. Box 79, 101 000 Moscow, USSR.
[14] Institut für Experimentelle Kernphysik, Universität Karlsruhe, Postfach 6980, D-7500 Karlsruhe 1, FRG
[15] High Energy Physics Laboratory, Institute of Nuclear Physics, Ul. Kawiory 26 a, PL-30055 Krakow 30, Poland
[16] Université de Paris-Sud, Lab. de l'Accélérateur Linéaire, Bat 200, F-91405 Orsay, France
[17] School of Physics and Materials, University of Lancaster - Lancaster LA1 4YB, UK
[18] LIP, Av. Elias Garcia 14 - 1e, P-1000 Lisbon Codex, Portugal
[19] Department of Physics, University of Liverpool, P.O. Box 147, GB - Liverpool L69 3BX, UK
[20] LPNHE, Universités Paris VI et VII, Tour 33 (RdC), 4 place Jussieu, F-75230 Paris Cedex 05, France
[21] Department of Physics, University of Lund, Sölvegatan 14, S-22363 Lund, Sweden
[22] Université Claude Bernard de Lyon, 43 Bd du 11 Novembre 1918, F-69622 Villeurbanne Cedex, France
[23] Universidad Complutense, Avda. Complutense s/n, E-28040 Madrid, Spain
[24] Univ. d'Aix - Marseille II - Case 907 - 70, route Léon Lachamp, F-13288 Marseille Cedex 09, France
[25] Dipartimento di Fisica, Università di Milano and INFN, Via Celoria 16, I-20133 Milan, Italy
[26] Niels Bohr Institute, Blegdamsvej 17, DK-2100 Copenhagen 0, Denmark
[27] NIKHEF-H, Postbus 41882, NL-1009 DB Amsterdam, The Netherlands
[28] National Technical University, Physics Department, Zografou Campus, GR-15773 Athens, Greece
[29] Physics Department, University of Oslo, Blindern, N-1000 Oslo 3, Norway
[30] Nuclear Physics Laboratory, University of Oxford, Keble Road, GB - Oxford OX1 3RH, UK
[31] Dipartimento di Fisica, Università di Padova and INFN, Via Marzolo 8, I-35131 Padua, Italy
[32] Rutherford Appleton Laboratory, Chilton, GB - Didcot OX11 OQX, UK
[33] Dipartimento di Fisica, Università di Roma II and INFN, Tor Vergata, I-00173 Rome, Italy
[34] CEN-Saclay, DPhPE, F-91191 Gif-sur-Yvette Cedex, France
[35] Istituto Superiore di Sanità, Ist. Naz. di Fisica Nucl. (INFN), Viale Regina Elena 299, I-00161 Rome, Italy
[36] Facultad de Ciencias, Universidad de Santander, av. de los Castros, E - 39005 Santander, Spain
[37] Inst. for High Energy Physics, Serpukow P.O. Box 35, Protvino, (Moscow Region), USSR.
[38] Institute of Physics, University of Stockholm, Vanadisvägen 9, S-113 46 Stockholm, Sweden
[39] Dipartimento di Fisica Sperimentale, Università di Torino and INFN, Via P. Giuria 1, I-10125 Turin, Italy
[40] Dipartimento di Fisica, Università di Trieste and INFN, Via A. Valerio 2, I-34127 Trieste, Italy
and Istituto di Fisica, Università di Udine, I-33100 Udine, Italy
[41] Department of Radiation Sciences, University of Uppsala, P.O. Box 535, S-751 21 Uppsala, Sweden
[42] Inst. de Fisica Corpuscular IFIC, Centro Mixto Univ. de Valencia-CSIC, and Departamento de Fisica Atomica Molecular y Nuclear, Univ. de Valencia, Avda. Dr. Moliner 50, E-46100 Burjassot (Valencia), Spain
[43] Institut für Hochenergiephysik, Österreich Akad. d. Wissensch., Nikolsdorfergasse 18, A-1050 Vienna, Austria
[44] Inst. Nuclear Studies and, University of Warsaw, Ul. Hoza 69, PL-00681 Warsaw, Poland
[45] Fachbereich Physik, University of Wuppertal, Postfach 100 127, D-5600 Wuppertal 1, FRG

1 Introduction

The forward backward asymmetry A_{FB} in $e^+e^- \to f\bar{f}$ ($f = \mu,\ e,\ \tau,\ q$) is sensitive to the axial- and vector-coupling of the initial and final state fermions. At $\sqrt{s} = M_Z$ it is described in lowest order by the relation :

$$A_{FB}^f = \frac{3}{4}\mathcal{A}_e\mathcal{A}_f$$

with

$$\mathcal{A}_f = \frac{2v_f a_f}{v_f^2 + a_f^2} = \frac{2(1 - 4|Q_f|\sin^2\theta_W)}{1 + (1 - 4|Q_f|\sin^2\theta_W)^2}$$

which is valid for light fermions $\left(\frac{m_f}{M_Z} \ll 1\right)$ and neglecting terms of the order $\left(\frac{\Gamma_Z}{M_Z}\right)^2$ for the γ-exchange. Results on A_{FB} for μ, e and τ final states have already be presented by the LEP collaborations [1].

In this paper the asymmetry for bottom quarks A_{FB}^b is determined by selecting their semileptonic decay into muons. The angular distribution of the b-quark in the reaction $e^+e^- \to b\bar{b}$ at $\sqrt{s} = M_Z$ is predicted by the Standard model to be :

$$\frac{d\sigma}{d\cos\theta_f} \propto \left(1 + \cos^2\theta_f + 2\cos\theta_f\mathcal{A}_e\mathcal{A}_f\right) = \left(1 + \cos^2\theta_f + \frac{8}{3}\cos\theta_f A_{FB}^b\right)$$

The line of flight of the b-quark is obtained from the direction of the event thrust axis, with orientation determined by the measured muon charge. The charge of the muon follows from the charge of the quark, up to $B^0\bar{B}^0$-mixing effects which can change the decay flavour content of the B-meson and thus fake the opposite direction. The muons produced by b-decay have large transverse momentum with respect to the jet axis. This allows the backgrounds from other channels to be reduced. To interpret the measured asymmetry in terms of the b-quark asymmetry, the flavour origin of muons as well as the hadronic background must be known.

2 The Detector

The DELPHI detector has been described in detail elsewhere [2]. Only components relevant to this analysis are summarized here. Charged particle tracks are reconstructed in a 1.23 T magnetic field, generated by a large superconducting solenoid. A time projection chamber is the main tracking device, which is supplemented in the barrel region by the inner detector and the outer detector. Two forward drift chambers complete the tracking system.

The iron return yoke of the magnet is instrumented with a hadron calorimeter segmented along its depth into four towers in both the barrel and the endcaps. The muon identification chambers are situated at the periphery of DELPHI after more than 1 m of iron. The barrel muon detector is divided into three layers: an inner, an external and a peripheral layer covering the dead space between sectors. Each layer consists of two active planes of drift chambers parallel to the beam axis measuring the transverse and longitudinal coordinates of the muon track. The forward muon detector consists of two

layers arranged in quadrants. Each layer contains two planes of drift chambers crossed at right angles, which measure the horizontal and vertical coordinates of the muon.

DELPHI is triggered by a redundant combination of signals from tracking chambers, electromagnetic calorimeters, muon chambers and scintillation hodoscopes in the barrel and forward region. The trigger efficiency for hadronic events is larger than 99 % for $|\cos\theta_{th}| < 0.93$, where θ_{th} is the polar angle of the thrust axis of the event.

3 Selection of hadronic Z°-events

The data used in this analysis have been collected during the year 1990 by DELPHI at the LEP collider. The sample of hadronic decays of the Z° is obtained with the following requirements :

a) at least 7 reconstructed charged particles coming from the interaction region with polar angle θ between 20^0 and 160^0 and momentum above 0.2 GeV/c

b) the total visible energy of charged and neutral particles has to be greater than 30 % of the centre of mass energy

c) the visible energy has to be at least 3 GeV in both the forward and backward hemispheres with respect to the beam axis

These cuts reduce the background (Z^0 leptonic decays, beam-gas events, $\gamma\gamma$-events) to less than 0.3 %. The efficiency of this selection is determined by Monte Carlo simulations to be about 93 % for hadronic Z°-decays. The identification of muons is essentially performed with the muon chambers in connection with the tracking devices in the barrel and in the forward region. In the analysis only data are retained taken in runs, where all necessary detectors were working well. In this way 79 271 events are selected with a centre of mass energy of $\sqrt{s} = M_Z \pm 0.2$ GeV.

4 Selection of muon candidates

The Z°$\rightarrow b\bar{b}$ channel is tagged by the identification of a muon coming from the semileptonic decay of a b- or $\bar{\text{b}}$-quark. Only particles with momentum larger than 3 GeV/c are considered, because the muons have to penetrate through the hadron calorimeter iron to the muon chambers.

To accept a track as a muon candidate a fit combining the muon chamber hits with the tracking information is performed. Therefore the tracks are extrapolated to the muon chambers and then associated and fitted to the muon chamber hits. The result of this procedure is a fitted track at the muon chambers and a χ^2. In the barrel region the following requirements must be fulfilled:

- There must be at least 2 planes hit in the muon chambers with at least one plane hit in one of the two external layers .

- The fit should have an acceptable χ^2, where the χ^2 is calculated from the difference in transverse position and azimuthal angle between the extrapolated trajectory and the fitted track.

In the forward region the following requirements must be fulfilled:

- There must be at least 2 planes hit in the forward muon chambers with at least one plane hit in the external layer.

- The fit should have an acceptable χ^2 per degree of freedom, where the χ^2 is calculated from a) the difference in position between the extrapolated trajectory and fitted track in the horizontal and vertical coordinates and in the azimuthal and polar angle and b) the difference between the fitted track and the hits in the muon chambers.

The values of the the χ^2 cut in the barrel and forward region were evaluated from the data and optimised to suppress background (punch through, decays etc.) while keeping a high muon identification efficiency.

The analysis is restricted to muons with a polar angle θ_μ such that:

$$0.03 < |\cos\theta_\mu| < 0.60$$
$$0.71 < |\cos\theta_\mu| < 0.93$$

in order to exclude regions with poor geometrical acceptance. The identification efficiency is determined to be $\varepsilon_\mu = 78 \pm 2\,\%$ inside the acceptance of the barrel and forward muon chambers for muons with momenta larger than $3\,\mathrm{GeV/c}$. This number is determined by Monte Carlo simulation and checked with data from the $Z^\circ \rightarrow \mu^+\mu^-$ channel. More details on muon identification can be found in reference [4].

With these criteria 6564 muon candidates were selected in the momentum range $3\,\mathrm{GeV/c} < p^\mu < 35\,\mathrm{GeV/c}$.

5 Analysis method

The experimental muon distribution was modeled by generating simulated events with the Lund parton shower program JETSET 7.2 [3] using string fragmentation. For b- and c-quarks the fragmentation is described by the Peterson function [5]

$$f(z) = \frac{z(1-z)^2}{[(z-1)^2 + \varepsilon z]^2}$$

where z is the fraction of the quark momentum carried by the hadron. The hardness of the fragmention is determined by the parameter ε. The mean scaled energy of B-hadrons $\langle x_E \rangle = 0.705 \pm 0.011$ as recently measured by the LEP-collaborations [6] can be translated to $\varepsilon = 0.005 \pm 0.002$ using the Lund parton shower program. This value is chosen for the analysis. The generated events were passed through the full DELPHI chain of simulation and reconstruction.

Knowledge of the composition of the identified muon sample is needed for the determination of the asymmetry. Therefore the Monte Carlo sample is divided into four classes:

1) f_b muons from direct b-decay ($b \to \mu$)

2) f_{bc} muons from b-cascade ($b \to c(\bar{c}) \to \mu$)

3) f_c muons from direct c-decay ($c \to \mu$)

4) f_{back} other background (e.g. *punch through hadrons, muons from decay* ...)

The first class includes a small contribution of the order of a few percent from the process $b \to \tau \to \mu$. The composition of the sample predicted by Monte Carlo simulation depends strongly on the momentum spectra of the muon candidates. The variables used in the analysis are the longitudinal momentum p_L and the transverse momentum p_T of the muon with respect to the jet axis, which is determined using the Lund cluster algorithm [3] for charged and neutral particles. The parameter for the cluster distance scale is chosen to be $D_{join} = 2.5\,\mathrm{GeV}/c$. For the calculation of the axis of the jet to which the muon belongs, the muon momentum is excluded. The jet axis reproduces the original B-hadron direction with an accuracy of about 2 degrees on Monte Carlo simulated events. The relative contributions of the four classes obtained by full detector simulation for different p_T-cuts are summarized in Table 1.

The charge of the muon in the semileptonic b-decay reflects the charge of the original quark. The direction of quarks in the centre of mass system is taken to be the thrust axis of charged and neutral particles in hadronic events. The orientation is then calculated by multiplying $-\cos\theta_{th}$ with the muon charge.

Source	*no* p_T *cut*	$p_T < 0.6\,\mathrm{GeV/c}$	$p_T > 0.7\,\mathrm{GeV/c}$	$p_T > 1.2\,\mathrm{GeV/c}$
f_b	27.2 %	4.5 %	44.2 %	61.9 %
f_{bc}	14.2 %	15.3 %	13.0 %	9.0 %
f_c	14.4 %	19.3 %	10.6 %	6.8 %
f_{back}	44.2 %	60.9 %	32.2 %	22.3 %

Table 1: Composition of the sample of muon candidates generated with the full DELPHI simulation, for muon momenta between 3 and 35 GeV/c.

6 Fitting procedures

The determination of the forward backward asymmetry A^b_{FB} has been performed using three different fitting procedures. The first one is an unbinned maximum likelihood fit to the p_L and p_T distribution of the muons with respect to the the thrust axis. To check the results of this fit a binned maximum likelihood fit to the same distribution is performed. As an independent analysis also a direct χ^2-fit to the angular distribution of muons after acceptance correction and background subtraction was done.

6.1 The unbinned maximum likelihood fit

A precise determination of the parameter A^b_{FB} is achieved by an unbinned maximum likelihood fit to the $\cos\theta_{th}$ distribution in the region $p^\mu > 3\,\mathrm{GeV/c}$ and $p^\mu_T > 0.7\,\mathrm{GeV/c}$

using the $p_L - p_T$ distribution to determine the different contributions coming from the 4 classes defined in section 5. The number of events selected within these kinematical cuts is 3226. Figures 1,2 and 3 compare the measured distributions of p, p_T and $-Q_\mu \cdot \cos\theta_{th}$ with the prediction from simulation, split into the different classes. The method has already been used in a similar way by the L3-collaboration [7]. First a distance is defined inside the momentum plane as follows :

$$\mathcal{D}_{1,2} = \sqrt{(\log p_{L,1} - \log p_{L,2})^2 + (e^{-p_{T,1}} - e^{-p_{T,2}})^2}$$

To calculate the probabilities that an event belongs to the different classes, Monte Carlo generated events close to the data event are used. For each event the N_{MC} Monte Carlo events with the smallest distance in the $\log p_L$ vs. e^{-p_T} plane are collected. Data events with a muon in the barrel (forward) muon chambers are compared only with Monte Carlo events with a muon in the barrel (forward) chambers respectively. The definition of the distance ensures that the density of simulated events around each data point is approximately constant. From the N_{MC} Monte Carlo events the probabilities that the event belongs to one of the four classes quoted in section 5 are calculated. For this analysis $N_{MC} = 40$ is chosen, which is a value optimized for the available statistics. It has been checked that for the present analysis the systematic bias of the fit result introduced by the fit procedure is less than one tenth of the statistical error. The statistical error of the Monte Carlo event sample is given in Table 2.

The asymmetry at a fixed polar angle θ_{th} determines the contribution to the log likelihood according to the different origin of muons :

$$F_k(\theta_{th}) = \frac{1}{2}\left(1 + \frac{8}{3} A_k \frac{\cos\theta_{th}}{1+\cos^2\theta_{th}}\right)$$

$$\begin{aligned} \text{with } A_1 &= A_{FB}^{b,exp} \\ A_2 &= A_{FB}^{bc,exp} = -c_1 A_{FB}^{b,exp} \\ A_3 &= A_{FB}^{c} = -c_2 A_{FB}^{b,exp} \\ A_4 &= 0 \end{aligned}$$

where A_k is the integrated asymmetry of class k and the superscript *'exp'* indicates that the experimental measured asymmetry is reduced by $B^0\bar{B}^0$-mixing. The additional factor c_1 has been calculated with the JETSET 7.2 Monte Carlo program. It is due to the fact that the b-quark may decay either into a c-quark or into a $\bar{c}$-quark. Because of the opposite charge sign of the produced muons, the contributions of these two different processes cancel partly. The correction factor c_2 has been calculated using KORAL-Z [8] ($\sin^2\theta_W = 0.23$) and correcting for $B^0\bar{B}^0$-mixing assuming $\chi = 0.143$ (see also section 7). On the Z^0-peak these factors are found to be :

$$c_1 = 0.77$$
$$c_2 = 0.88$$

The asymmetry of the background A_4 is calculated with the Monte Carlo simulation and is compatible with zero. Due to the $\cos\theta_{th}$ dependence of the thickness of penetrated iron inside the detector the background fraction depends on the polar angle of the muon. To take this into account the Monte Carlo ratio of background to true muons was fitted as a polynomial in $\cos\theta_{th}$. The background events have been reweighted according to their

polar angle keeping the total number constant. No $\cos\theta_{th}$ dependence was found for the ratios of the other classes .

Combining all information gives the negative logarithm of the likelihood function, which has to be minimized :

$$\mathcal{L} = -\log\left(\prod_{j=1}^{N_{data}} \sum_{k=1}^{4} p_{k_j} F_k(\theta_{th}^j)\right),$$

where p_{k_j} is the probability of event j to belong to class k as determined from the N_{MC} Monte Carlo events around event j.

The fitted asymmetry for the sample is :

$$A_{FB}^{b,exp} = 0.115 \pm 0.043\,(stat) \pm 0.013\,(syst)$$

The statistical uncertainty comes from the fit, while the contributions to the total systematic uncertainty shown are detailed in Table 2. These contributions have been studied and evaluated in the ranges given.

	range	$\pm\Delta A_{FB}^{b,exp}$
Variation of the Peterson fragmentation parameter ε_b	0.003-0.007	0.007
Variation of the b-cascade fraction	(0.80-1.20)$\cdot f_{bc}$	0.001
Variation of the c-quark fraction	(0.89-1.11)$\cdot f_c$	0.001
Variation of the total background fraction	(0.90-1.10)$\cdot f_{back}$	0.002
Variation of the background fraction in the endcap region	(0.50-1.50)$\cdot f_{back}^{forw}$	0.006
Variation of the factor c_1 for different b-cascade contributions	0.5-1.0	0.002
Variation of the factor c_2 for the c-quark asymmetry	0.6-1.1	0.005
Transverse momentum smearing with respect to the beam axis by $\Delta p = 0.01 \cdot p^2$		0.001
Fit method (definition of the distance, number of Monte Carlo events collected)		0.005
Statistical error of the Monte Carlo sample		0.006
Total		0.013

Table 2: Contributions to the systematic error of the maximum likelihood fit

6.2 The binned maximum likelihood fit

A binned maximum likelihood fit in the 2-dimensional p_L-p_T-distribution has been performed to obtain the asymmetry of the b-quark. The method is based on counting the number of events in the forward and backward hemispheres with respect to the initial electron direction. The asymmetry is then determined from:

$$A_{FB}^{b,exp} = \frac{N^{forw} - N^{back}}{N^{forw} + N^{back}}$$

All muon candidates with $p_T > 0.7\,\mathrm{GeV/c}$ are weighted according to:

$$F_k = \frac{1}{2}(1 \pm A_k)$$

where the +/- sign is used for events in forward and backward hemispheres. The likelihood function is defined as above where the probability p_{k_j} is evaluated in each bin of p_L, p_T. In the fit the values for A_k are taken to be the same as above and the b-quark asymmetry is left free. The asymmetry becomes:

$$A_{FB}^{b,exp} = 0.108 \pm 0.048\,(stat) \pm 0.013\,(syst)$$

which is consistent with the result obtained with the unbinned maximum likelihood fit.

6.3 The χ^2-fit

The unbinned maximum likelihood fit is considered to be the most precise method for the determination of the asymmetry due to the construction of the likelihood function. On the other hand the understanding of the acceptance and the background can be proved performing a conventional least square fit to the angular distribution, where the evaluation of the quality of the fit is given by the χ^2 value. The distribution of the polar angle of the thrust axis is directly compared with the prediction of the Standard model :

$$\frac{d\sigma}{d\cos\theta_{th}} \propto \left[1 + \cos^2\theta_{th} + \frac{8}{3} A_{FB}^{obs} \cos\theta_{th}\right]$$

To enrich the sample of b-quark candidates a more severe cut on the transverse momentum of $p_T > 1.2\,\mathrm{GeV/c}$ is performed. This reduces the number of events with identified muons to 1714. The sample includes contributions from b-cascade, charmed quarks, misidentified hadrons and decays. In this kinematical region the latter two amount to a fraction of 22 %. The background contribution can be checked with muon candidates which have $p_T < 0.6\,\mathrm{GeV/c}$. In this region the background is expected to be dominant (see Table 1) and the asymmetry, obtained by counting the backward and forward events, is found to be $A_{FB}^{back} = 0.005 \pm 0.020$.

After hadronic background subtraction and acceptance correction the expression quoted above has been fitted to the data using a conventional χ^2-fit method with the asymmetry as a free parameter. The angular domain of the thrust axis is restricted to $|\cos\theta_{th}| < 0.90$. The result of the fit gives the observed asymmetry :

$$A_{FB}^{obs} = 0.073 \pm 0.039 \quad \text{with } \chi^2 = 11.0 \text{ for 16 degrees of freedom}$$

The angular distribution and the result of the fit are shown in figure 4. The observed asymmetry is related to the b-asymmetry as follows :

$$A_{FB}^{obs} = f_b' A_{FB}^{b,exp} + f_c' A_{FB}^{c} + f_{bc}' A_{FB}^{bc}$$

with

$$f_i' = \frac{f_i}{f_b + f_{bc} + f_c}$$

The asymmetry of the b-cascade and of the c-quark is again assumed to be :

$$A_{FB}^{bc} = -c_1 A_{FB}^{b,exp} \quad \text{and} \quad A_{FB}^{c} = -c_2 A_{FB}^{b,exp}$$

using the same values for c_1 and c_2 as quoted before. Extracting the fractions f_b', f_{bc}' and f_c' from Monte Carlo simulation leads to :

$$A_{FB}^{b,exp} = 0.116 \pm 0.062\,(stat) \pm 0.021\,(syst)$$

This result is consistent with the previous estimates. It has however larger statistical errors due to the higher p_t cut and to the background and acceptance corrections. The systematic error has been evaluated varying the fractions f_i of the different muon sources and the values of c_1 and c_2 in the ranges of Table 2. This gives a contribution of the fractions of 0.020 and of the factors of 0.004 and 0.005 respectively.

7 Extraction of the electroweak mixing angle

The relation between the quark and the measured asymmetry is sensitive to the mixing in the $B_d^0\bar{B}_d^0$- and $B_s^0\bar{B}_s^0$-system. Therefore the experimentally determined asymmetry has to be corrected by a factor $(1-2\chi)^{-1}$, where χ gives the probability that the neutral B-meson has changed its flavour content. For the mixing parameter the average value measured at LEP-energies [6] is used

$$\chi_{LEP} = 0.143 \pm 0.023$$

where the natural mixture of the different B-hadrons produced at the Z°are included. The result of the unbinned maximum likelihood fit, which yields the smallest error, increases to a value of

$$A_{FB}^{b} = \frac{A_{FB}^{b,exp}}{(1-2\chi_{LEP})} = 0.161 \pm 0.060\,(stat) \pm 0.018\,(syst) \pm 0.010\,(syst)$$

The last contribution of the error is due to the uncertainty of the mixing parameter. Using the program ZFITTER [9], which includes QED radiative corrections, the electroweak mixing angle in the $\overline{\rm MS}$ renormalisation scheme is determined to be :

$$\sin^2\theta_{\rm W}^{\overline{\rm MS}} = 0.221 \pm 0.011\,(stat) \pm 0.003\,(syst) \pm 0.002\,(syst)$$

The result agrees with the values determined from $b\bar{b}$-asymmetries by the other LEP collaborations [7,10] and also with those obtained from di-lepton asymmetries and Z°-lineshape measurements [11].

Acknowledgements

We are greatly indebted to our technical collaborators and to the funding agencies for their support in building and operating the DELPHI detector, and to the members of the CERN-SL Division for the excellent performance of the LEP collider.

References

[1] The ALEPH Collaboration, D.Decamp et al., *Improved measurements of electroweak parameters from Z^0 decays into fermion pairs*, CERN PPE/91-105 to be published in Zeit. Phys.C;
The DELPHI Collaboration, P.Abreu et al., *Determination of Z^0 resonance parameters and couplings from its hadronic and leptonic decays*, CERN PPE/91-95 to be published in Nucl. Phys;
The L3 Collaboration, B.Adeva et al., Zeit. Phys. C51 (1991) 179;
The OPAL Collaboration, M.Z.Akrawy et al., Zeit. Phys. C52 (1991) 175.

[2] The DELPHI Collaboration, P. Aarnio et al., Nucl. Instrum. Methods A303 (1991) 233.

[3] T.Sjöstrand et al. Comp. Phys. Comm. 39 (1986) 346 and Comp. Phys. Comm. 43 (1987) 347.

[4] The DELPHI collaboration, P Abreu et al., *Measurement of the partial width of the Z^0 into $b\bar{b}$ final states and of the mean B semileptonic branching fraction*, To be published.

[5] C.Peterson et al., Phys. Rev. D27 (1983) 105.

[6] P.Roudeau, *Heavy Quark Physic at LEP*, Joint Int. Lepton-Photon Symp. and Europhys. Conf. on High Energy Physics 1991.

[7] The L3 Collaboration, B. Adeva et al., Phys. Lett. B238 (1990) 122, and B252 (1990) 713.

[8] S.Jadach, Z.Was, *The Monte Carlo program KORALZ*, CERN TH 5994-91 (1991).

[9] D.Bardin et al., Zeit. Phys. C44 (1989) 493, Comp. Phys. Comm. 59 (1990) 303, Nucl. Phys. B351 (1991) 1.

[10] The ALEPH Collaboration, D.Decamp et al., Phys. Lett. B263 (1991)325;
The OPAL Collaboration, M.Z. Akrawy et al., Phys. Lett. B263 (1991) 311.

[11] J.R.Carter, *Precision tests of the Standard model at LEP*, Joint Int. Lepton-Photon Symp. and Europhys. Conf. on High Energy Physics 1991.

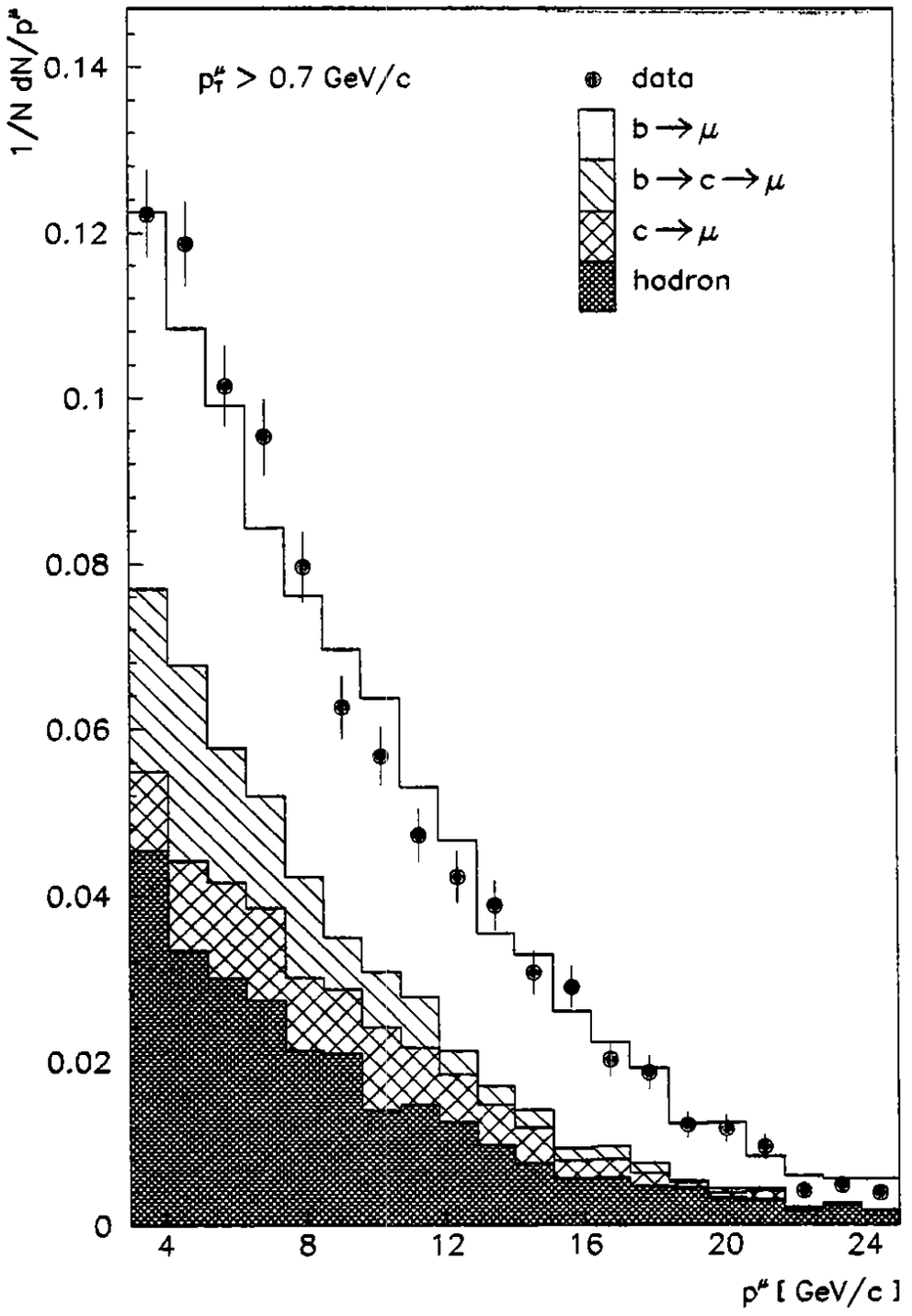

Figure 1: Momentum distribution of accepted muons compared to simulation separated into different classes

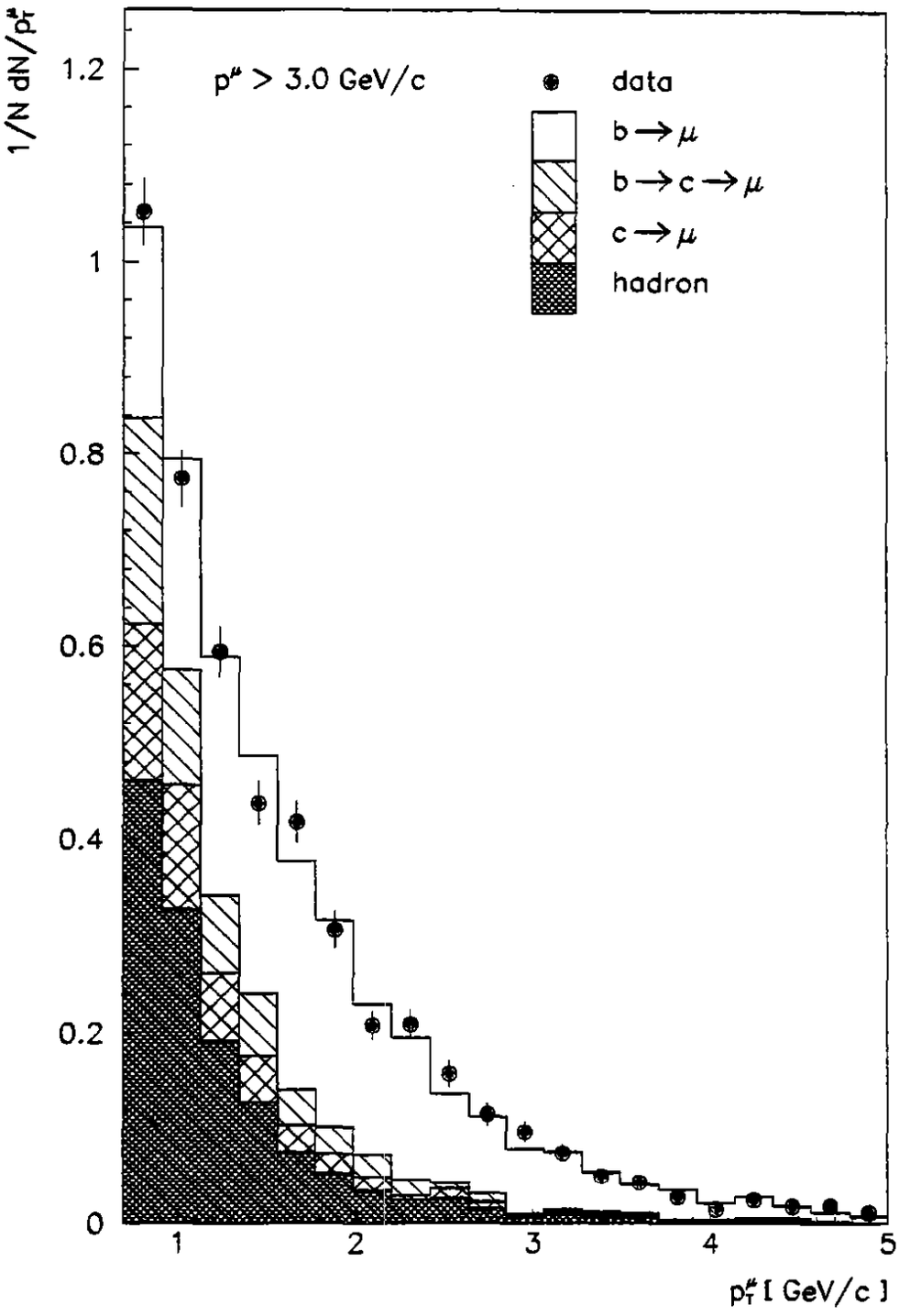

Figure 2: Transverse momentum distribution of accepted muons compared to simulation separated into different classes

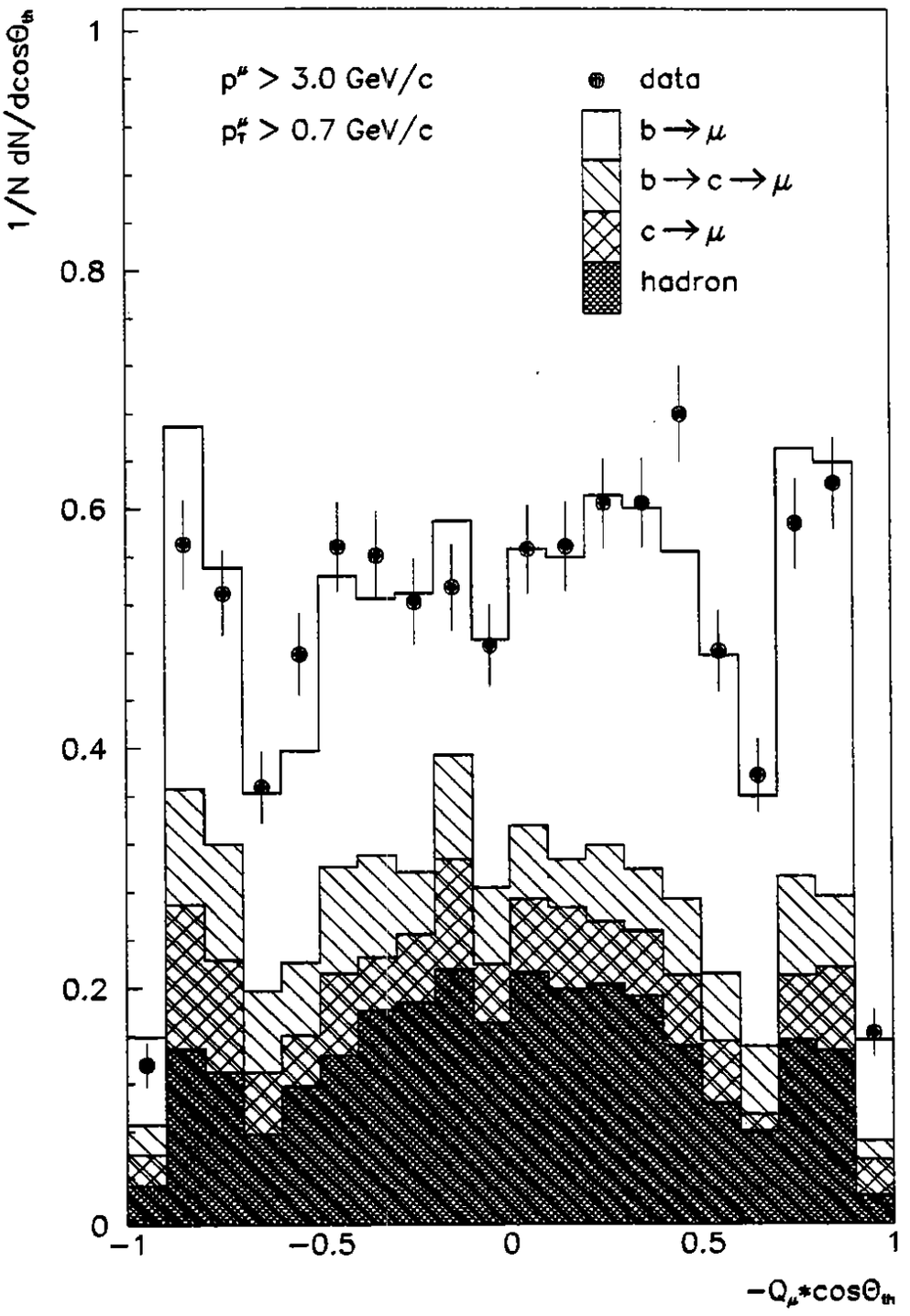

Figure 3: Polar angle distribution of the thrust axis multiplied by the muon charge compared to simulation separated into different classes

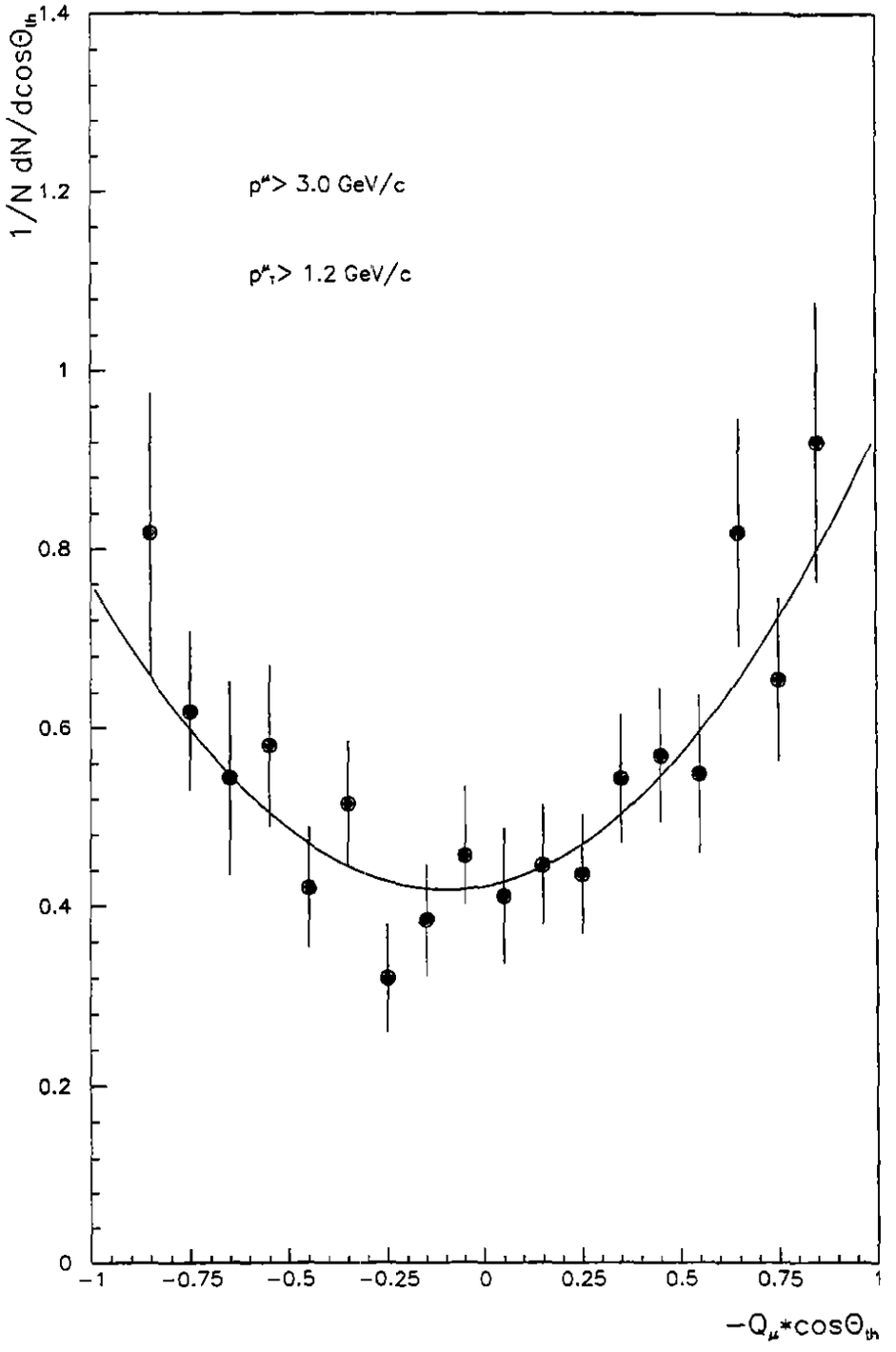

Figure 4: Polar angle distribution after background subtraction and efficiency correction, the solid curve is obtained from the χ^2-fit to the cosine theta distribution of the data

Imprimé au CERN. Prix: 0.55 Fr.